

Tyrosinase Reactivity in a Model Complex: An Alternative Hydroxylation Mechanism

Liviu M. Mirica,¹ Michael Vance,¹ Deanne Jackson Rudd,¹
Britt Hedman,^{2*} Keith O. Hodgson,^{1,2*} Edward I. Solomon,^{1*}
T. Daniel P. Stack^{1*}

The binuclear copper enzyme tyrosinase activates O₂ to form a μ - η^2 : η^2 -peroxodicopper(II) complex, which oxidizes phenols to catechols. Here, a synthetic μ - η^2 : η^2 -peroxodicopper(II) complex, with an absorption spectrum similar to that of the enzymatic active oxidant, is reported to rapidly hydroxylate phenolates at -80°C . Upon phenolate addition at extreme temperature in solution (-120°C), a reactive intermediate consistent with a bis- μ -oxodicopper(III)-phenolate complex, with the O–O bond fully cleaved, is observed experimentally. The subsequent hydroxylation step has the hallmarks of an electrophilic aromatic substitution mechanism, similar to tyrosinase. Overall, the evidence for sequential O–O bond cleavage and C–O bond formation in this synthetic complex suggests an alternative intimate mechanism to the concerted or late stage O–O bond scission generally accepted for the phenol hydroxylation reaction performed by tyrosinase.

Tyrosinase is a ubiquitous binuclear copper enzyme, found in fungi, plants, and animals, that catalyzes the hydroxylation of phenols to catechols and the oxidation of catechols to quinones (1). The oxygenated form of tyrosinase contains a μ - η^2 : η^2 -peroxodicopper(II) species (P in Scheme 1), with an intact O–O bond, that hydroxylates phenols through a mechanism consistent with an electrophilic aromatic substitution. Because intermediates beyond the P species are unknown, the sequence of intimate steps of bond cleavage and formation remains unclear. Nonetheless, the electrophilic character of the enzymatic reaction suggests a mechanism, generally accepted, in which the O–O bond cleavage occurs either concerted with or after C–O bond formation (2, 3).

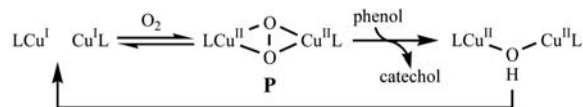
The impressive C–H oxidation by tyrosinase has elicited extensive synthetic efforts to create copper complexes that not only react with O₂ to form spectroscopically faithful P model complexes (4) but also oxidize C–H bonds (5). Though many synthetic P analogs are known, only a limited number function as hydroxylating agents of externally added phenolate substrates (6–8). Compared with biological systems (9–11), the low temperatures and aprotic solvents tolerated by synthetic systems provide potential advantages in detection and characterization of reactive intermediates.

¹Department of Chemistry, Stanford University, CA 94305, USA. ²Stanford Synchrotron Radiation Laboratory, Stanford Linear Accelerator Center, Stanford University, CA 94309, USA.

*To whom correspondence should be addressed. E-mail: stack@stanford.edu (T.D.P.S.); edward.solomon@stanford.edu (E.I.S.); hodgson@ssrl.slac.stanford.edu (K.O.H.); hedman@ssrl.slac.stanford.edu (B.H.)

Here, we report the stabilization at -120°C of an intermediate formed in the reaction of a synthetic P species with an added phenolate. Spectroscopic characterization indicates a bis- μ -oxodicopper(III)-phenolate complex in which the O–O bond is cleaved and the phenolate is ligated to a copper center. This intermediate decays slowly at -120°C to hydroxylate the aromatic ring through a step that exhibits the hallmarks of an electrophilic aromatic substitution reaction (7). The data, in accord with density functional theory (DFT) calculations, strongly support this bis- μ -oxodicopper(III) species as an electrophilic oxidation agent in the hydroxylation reaction. As such, this study provides experimental evidence for an alternative hydroxylation mechanism for the μ - η^2 : η^2 -peroxodicopper(II) species in tyrosinase, entailing O–O bond cleavage prior to C–O bond formation (12).

The reaction of the copper(I) complex of *N,N'*-di-*tert*-butyl-ethylenediamine



Scheme 1.

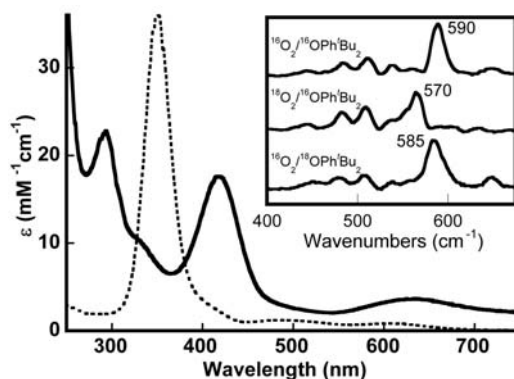


Fig. 1. UV-Vis spectrum of A (solid line) and pDBED (dashed line) in MeTHF (153 K, [Cu] \approx 1 mM). Inset: Resonance Raman spectra of A (λ_{ex} = 413 nm, MeTHF, 77 K, [Cu] \approx 1 mM) with $^{16}\text{O}_2/^{16}\text{OPh}^t\text{Bu}_2$ (top line), $^{18}\text{O}_2/^{16}\text{OPh}^t\text{Bu}_2$ (middle line), or $^{16}\text{O}_2/^{18}\text{OPh}^t\text{Bu}_2$ (bottom line).

(DBED) with O₂ at -80°C in aprotic solvents (tetrahydrofuran, CH₂Cl₂, or acetone) generates a μ - η^2 : η^2 -peroxodicopper(II) complex, pDBED, identified by its characteristic absorption band (350 nm, ϵ = 36 mM⁻¹ cm⁻¹), resonance Raman stretch [$\nu_{\text{O-O}} = 721 \text{ cm}^{-1}$, $\Delta(^{18}\text{O}_2) = 40 \text{ cm}^{-1}$], and a Cu \cdots Cu distance of 3.45 Å (8), similar to other characterized P complexes (4). pDBED reacts rapidly at -80°C with 1 equivalent of sodium 2,4-di-*tert*-butylphenolate, without the appearance of any intermediate species, to yield an \sim 1:1 mixture of 3,5-di-*tert*-butylcatechol and 3,5-di-*tert*-butyl-1,2-benzoquinone (Scheme 2). The product yield accounts for \sim 90% of the oxidizing equivalents of pDBED, and one oxygen atom is transferred from pDBED to the phenyl ring, as assessed by $^{18}\text{O}_2$ substitution (8). pDBED reacts more slowly with more electron-deficient phenolates (13), consistent with an electrophilic aromatic substitution mechanism.

At lower temperature (-120°C) in 2-methyltetrahydrofuran (MeTHF), pDBED reacts with sodium 2,4-di-*tert*-butylphenolate to form a transient intermediate A that exhibits distinct intense absorption features (Fig. 1). Full formation requires the addition of at least three equivalents of this phenolate at millimolar concentrations. Optical titrations of pDBED with sodium 2,4-di-*tert*-butylphenolate support the formation of a 1:1 complex with a binding constant of 16,000 M⁻¹ ($\log K \approx 4.2$) (14). Compound A decays by a first-order process ($t_{1/2} = 38 \text{ min}$, -120°C), and the resulting solution has an absorption spectrum and hydroxylated product yield nearly identical to those of the reaction performed at -80°C (15). The intense charge-transfer band of A at 418 nm ($\epsilon = 18 \text{ mM}^{-1} \text{ cm}^{-1}$) is reminiscent of a bis- μ -oxodicopper(III) complex, a species that is now extensively characterized with a wide variety of neutral and anionic ligands (4, 16–18). The less intense visible absorption band at 630 nm is assigned to a phenolate-to-Cu charge-

transfer transition (19). Resonance Raman experiments ($\lambda_{\text{exc}} = 413 \text{ nm}$) reveal a bis- μ -oxodicopper(III) Cu_2O_2 core stretch at 590 cm^{-1} that shifts by 20 cm^{-1} upon $^{18}\text{O}_2$ substitution (20, 21). On addition of ^{18}O -2,4-di-*tert*-butylphenolate, the 590 cm^{-1} stretch shifts by 5 cm^{-1} (Fig. 1, inset). The appreciable coupling of the Cu_2O_2 core and Cu-phenolate vibrations is only possible with a direct interaction of the phenolate ligand with the copper complex in **A**. A Hammett parameter of $\rho = -2.2$, determined for the decay of a series of **A** complexes with more electron-deficient phenolates at -120°C (Fig. 2), supports an electrophilic aromatic substitution mechanism; the value for tyrosinase is $\rho = -2.4$ (22). Further support for this mechanism is provided by the measured inverse secondary C-H/C-D kinetic isotope effect of 0.83 ± 0.09 on the decay rate of species **A** with 2,4-di-*tert*-butyl-6-H(D)-phenolate at -105°C (14).

Solution Cu K-edge x-ray absorption spectroscopy (XAS) on **A** in MeTHF exhibits two very weak pre-edge features at 8979 and 8980.5 eV, the latter of which is characteristic of a Cu(III) center (23, 24). All fits to the extended x-ray absorption fine structure (EXAFS) data required a Cu...Cu contribution at 2.79 \AA (14), a distance consistent with other structurally characterized bis- μ -oxodicopper(III) complexes (4), and each Cu coordination is best fit with four N/O ligands (25) at an average distance of 1.89 \AA (Fig. 3).

The presented experimental evidence thus supports a bis- μ -oxodicopper(III)-phenolate structure for **A** (Scheme 2). Equatorial phenolate ligation, at the expense of the positioning of one of the amine groups of DBED axially, would be expected to enhance the relative stability of Cu(III) (4). It is well documented that the energy difference of the Cu(II) μ - η^2 : η^2 -peroxodicopper(II) and Cu(III) bis- μ -oxodicopper(III) isomers with sterically demanding neutral ligands such as DBED can be small at low temperatures (4, 5, 26). This near isoenergetic relation is biased toward the higher oxidation state by the addition of an anionic ligand. The DFT geometry-optimized

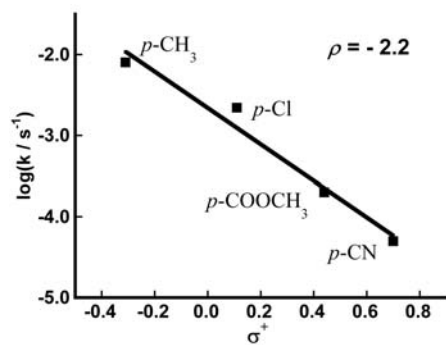
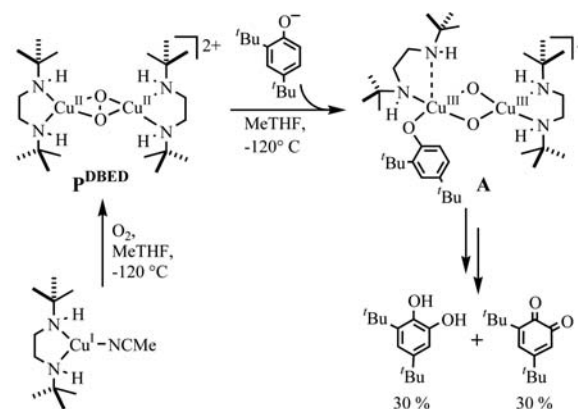


Fig. 2. A Hammett plot of the thermal decay of species **A** at -120°C ($\rho = -2.2$). The para-substituted phenolates used are indicated on the plot.

structure of **A**, which included the entire monocationic complex, supports an electronic preference for the equatorial positioning of the phenolate ligand and predicts Cu...Cu (2.76 \AA) and Cu-O/ N_{ave} (1.88 \AA) distances in good agreement with the EXAFS data (14).

On the basis of the present investigation, the hydroxylation of phenolate by **PDBED** through the intermediacy of **A** has the characteristics of an electrophilic aromatic substitution reaction, which is intriguing because such bis- μ -oxodicopper(III) species are generally not considered to be electrophiles (4, 26, 27). A frontier molecular orbital analysis of the electronic ground state of the DFT-optimized structure of **A** suggests that the equatorial positioning of the phenolate provides an almost ideal geometry for a perpendicular σ -attack of the phenolate-based π highest occupied molecular orbital (HOMO) on the Cu_2O_2 -based σ^* lowest unoccupied molecular orbital (LUMO) (Fig. 4) (12, 28, 29). Moreover, the activation energy (10.9 kcal/mol at -120°C) calculated by DFT for the phenolate hydroxylation step of the **A** species agrees well with the experimental activation energy value of $\sim 10.3 \text{ kcal/mol}$ (14), which supports this pathway as an energetically viable reaction coordinate for hydroxylation.

The associative rearrangement of the anionic ligand into



Scheme 2.

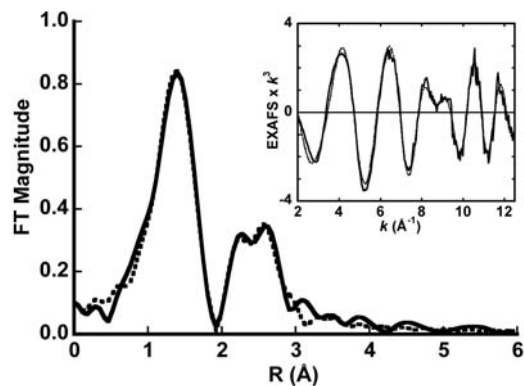


Fig. 3. Non-phase-shift corrected Fourier transform of EXAFS data (solid line) and four-coordinate fit (dashed line) of **A** (MeTHF, 10 K, $[\text{Cu}] \approx 1 \text{ mM}$). (Inset) The EXAFS data (solid line) and four-coordinate fit (dashed line).

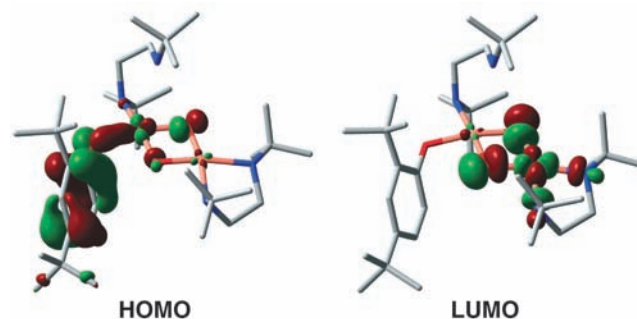


Fig. 4. Spatial representation of HOMO [(left) phenolate π orbital] and LUMO [(right) Cu_2O_2 core σ^* orbital], calculated for the DFT geometry-optimized model of **A**, showing the favorable σ -attack conformation. The orbital contour was set at $0.05 \text{ e}^-/\text{\AA}^3$.

References and Notes

- E. I. Solomon, U. M. Sundaram, T. E. Machonkin, *Chem. Rev.* **96**, 2563 (1996).
- H. Decker, R. Dillinger, F. Tuzcek, *Angew. Chem. Int. Ed. Engl.* **39**, 1591 (2000).
- S. Mandal, D. Macikenas, J. D. Protasiewicz, L. M. Sayre, *J. Org. Chem.* **65**, 4804 (2000).
- L. M. Mirica, X. Ottenwaelder, T. D. P. Stack, *Chem. Rev.* **104**, 1013 (2004).
- E. A. Lewis, W. B. Tolman, *Chem. Rev.* **104**, 1047 (2004).
- L. Santagostini *et al.*, *Chem. Eur. J.* **6**, 519 (2000).
- S. Itoh *et al.*, *J. Am. Chem. Soc.* **123**, 6708 (2001).
- L. M. Mirica *et al.*, *J. Am. Chem. Soc.* **124**, 9332 (2002).
- M. Kim *et al.*, *Nat. Struct. Biol.* **9**, 591 (2002).
- J. C. Price, E. W. Barr, B. Tirupati, J. M. Bollinger, C. Krebs, *Biochemistry* **42**, 7497 (2003).
- M. T. Green, J. H. Dawson, H. B. Gray, *Science* **304**, 1653 (2004).
- Note that a synthetic $\mu\text{-}\eta^2\text{-}\eta^2\text{-peroxodicopper(II)}$ complex has been shown to directly hydroxylate an aromatic ring on a noncoordinating substrate (32).
- A lower yield of the products is observed for electron-deficient substrates.
- Materials and methods are available as supporting material on Science Online.
- Both catechol and quinone are produced upon acidic workup of the solution mixture, which supports A as a reactive species during hydroxylation.
- J. A. Halfen *et al.*, *Science* **271**, 1397 (1996).
- S. Mahapatra, V. G. Young, S. Kaderli, A. D. Zuberbühler, W. B. Tolman, *Angew. Chem. Int. Ed. Engl.* **36**, 130 (1997).
- V. Mahadevan *et al.*, *J. Am. Chem. Soc.* **119**, 11996 (1997).
- A resonance Raman spectrum resulting from 600-nm excitation shows a C–O stretch at 1280 cm^{-1} , which supports a phenolate to Cu charge-transfer assignment.
- M. J. Henson, P. Mukherjee, D. E. Root, T. D. P. Stack, E. I. Solomon, *J. Am. Chem. Soc.* **121**, 10332 (1999).
- No vibrations characteristic for P complex (at ~ 300 or ~ 730 cm^{-1}) are observed.
- S. Yamazaki, S. Itoh, *J. Am. Chem. Soc.* **125**, 13034 (2003).
- J. L. DuBois *et al.*, *J. Am. Chem. Soc.* **119**, 8578 (1997).
- J. L. DuBois *et al.*, *J. Am. Chem. Soc.* **122**, 5775 (2000).
- EXAFS analysis typically cannot distinguish between atoms that differ in Z by 1 (e.g., O and N) (33). Given the k range of the EXAFS data ($k = 3$ to 12.5 \AA^{-1}), any difference in R less than 0.17 \AA between ligands in the first coordination shell (at 1.89 \AA) could not be resolved.
- V. Mahadevan, M. J. Henson, E. I. Solomon, T. D. P. Stack, *J. Am. Chem. Soc.* **122**, 10249 (2000).
- An electrophilic aromatic substitution mechanism for a bis- $\mu\text{-oxodicopper(III)}$ complex has been proposed in a case in which a ligand aryl group is hydroxylated (34).
- P. Chen, E. I. Solomon, *J. Inorg. Biochem.* **88**, 368 (2002).
- E. I. Solomon, P. Chen, M. Metz, S.-K. Lee, A. E. Palmer, *Angew. Chem. Int. Ed. Engl.* **40**, 4570 (2001).
- D. E. Wilcox *et al.*, *J. Am. Chem. Soc.* **107**, 4015 (1985).
- P. E. M. Siegbahn, *J. Biol. Inorg. Chem.* **8**, 567 (2003).
- E. Pidcock, H. V. Obias, C. X. Zhang, K. D. Karlin, E. I. Solomon, *J. Am. Chem. Soc.* **120**, 7841 (1998).
- R. A. Scott, *Methods Enzymol.* **117**, 414 (1985).
- P. L. Holland, K. R. Rodgers, W. B. Tolman, *Angew. Chem. Int. Ed. Engl.* **38**, 1139 (1999).
- We thank R. Pratt for assistance in the synthesis of ^{18}O -di-*t*-butyl-phenolate and J. I. Brauman for insightful discussions. L.M.M. gratefully acknowledges a John Stauffer Stanford Graduate Fellowship. Funding was provided by NIH GM50730 (T.D.P.S), NIH DK31450 (E.I.S.), and NIH RR01209 (K.O.H.). XAS data were measured at the Stanford Synchrotron Radiation Laboratory (SSRL), which is supported by the Department of Energy, Office of Basic Energy Sciences. The SSRL Structural Molecular Biology program is funded by the National Institutes of Health, National Center for Research Resources, Biomedical Technology Program, and the Department of Energy, Office of Biological and Environmental Research.

Supporting Online Material

www.sciencemag.org/cgi/content/full/308/5730/1890/DC1
 Materials and Methods
 SOM Text
 Figs. S1 to S8
 Tables S1 to S3
 References

10 March 2005; accepted 10 May 2005
 10.1126/science.1112081

Sound Velocities of Hot Dense Iron: Birch's Law Revisited

Jung-Fu Lin,^{1*} Wolfgang Sturhahn,² Jiyong Zhao,² Guoyin Shen,³ Ho-kwang Mao,¹ Russell J. Hemley¹

Sound velocities of hexagonal close-packed iron (hcp-Fe) were measured at pressures up to 73 gigapascals and at temperatures up to 1700 kelvin with nuclear inelastic x-ray scattering in a laser-heated diamond anvil cell. The compressional-wave velocities (V_p) and shear-wave velocities (V_s) of hcp-Fe decreased significantly with increasing temperature under moderately high pressures. V_p and V_s under high pressures and temperatures thus cannot be fitted to a linear relation, Birch's law, which has been used to extrapolate measured sound velocities to densities of iron in Earth's interior. This result means that there are more light elements in Earth's core than have been inferred from linear extrapolation at room temperature.

The properties of Earth's iron-rich core have been inferred from estimates of iron density at high pressures and temperatures and from measurements of compressional-wave (V_p) and shear-wave (V_s) velocities passing through the core (1–13). These data have indicated that Earth's core is less dense than pure iron by approximately 10% for the outer core and 3% for the inner core, suggesting the existence of light elements in the core. On the other hand, Birch's law, a linear sound

velocity–density relation (2, 14, 15), has also been used to extrapolate measured sound velocities at high pressures and room temperatures to inner core conditions without considering the temperature effect (9, 12). This linear extrapolation has suggested that the inner core is mainly made of Fe–Ni alloy. The nuclear-resonant inelastic x-ray scattering (NRIXS) technique provides a direct probe of the phonon density of states (DOS) of the resonant isotope (16–18) using the 14.4125-keV transition of ^{57}Fe . V_p and V_s of hexagonal close-packed (hcp) Fe have been measured up to 153 GPa at 300 K (10, 19). However, the effect of temperature on the sound velocity measurements of Fe in static studies is not well understood. Here we report the static NRIXS study of the sound velocities of hcp-Fe up to 73 GPa and 1700 K in a laser-heated diamond anvil cell (LHDAC), and we

discuss the temperature effect on the sound velocities and Birch's law.

We conducted NRIXS experiments in an LHDAC at Sector 3 of the Advanced Photon Source (APS) at Argonne National Laboratory (20, 21). Energy spectra were obtained by tuning the x-ray energy (± 70 meV) around the nuclear transition energy of 14.4125 keV and collecting the Fe K-fluorescence (the emission of an x-ray photon via the transition of an atomic electron into an unoccupied 1s state) radiation that was emitted with time delay relative to the incident x-ray pulses. We used a quasiharmonic model to extract the phonon DOS from the NRIXS spectra (Fig. 1) according to the procedure described in (16–18). With the NRIXS technique, we measured the spectrum of the self-correlation function of the position of the Fe atoms (17). In the model, the atomic motions relative to the temperature-dependent averaged position are assumed to be harmonic under the given conditions of pressure, temperature, and other parameters. Thermal effects, such as expansion and change of force constants with atomic distances, were allowed to change but the vibrations were still assumed to occur in a harmonic potential. The average kinetic energy and force constant independently derived from the moments of the measured spectra were consistent with the values evaluated from the quasiharmonic model (17), indicating the validity of the model to our high-pressure/temperature data (22). The Debye sound velocity (V_D) was derived from parabolic fitting of the low-energy regime of the DOS (16–18), and the vibrational, elastic, and thermodynamic parameters were obtained by the integration of the DOS. We then calculated the thermal

¹Geophysical Laboratory, Carnegie Institution of Washington, 5251 Broad Branch Road, N.W., Washington, DC 20015, USA. ²Advanced Photon Source, Argonne National Laboratory, 9700 South Cass Avenue, Argonne, IL 60439, USA. ³Consortium for Advanced Radiation Sources, The University of Chicago, Chicago, IL 60637, USA.

*To whom correspondence should be addressed. E-mail: j.lin@gl.ciw.edu